June 1974

LRP 83/74

A NEW FINITE ELEMENT APPROACH TO THE NORMAL MODE ANALYSIS IN MAGNETOHYDRODYNAMICS

K. Appert, D. Berger, R. Gruber, J. Rappaz

C R P P

Ecole Polytechnique Fédérale de Lausanne

June 1974

LRP 83/74

A NEW FINITE ELEMENT APPROACH TO THE NORMAL MODE ANALYSIS IN MAGNETOHYDRODYNAMICS

K. Appert, D. Berger, R. Gruber, J. Rappaz

Abstract

The eigenvalue problem arising in the one-dimensional normal mode analysis of fixed boundary magnetohydrodynamic stability is solved by a finite element method. Piecewise constant, discontinuous basis functions are used for two components of the displacement vector because this permits an accurate representation of the nearly divergence-free property of the modes being treated. In spite of the simple basis functions, the accuracy is greatly improved compared to that obtained with piecewise linear, continuous basis functions. Important features of the spectrum, such as infinitely degenerated eigenvalues, accumulation points and continua are well represented by the method. The method used should equally well be applicable to the free boundary stability problem.

Lausanne

INTRODUCTION

The finite element method was recently proposed by Ohta et al.[1] as a tool for the analysis of magnetohydrodynamic stability of a current-carrying plasma. Since then several authors [2, 3, 4] have applied the method to infinitely long, axisymmetric plasmas. The problem to be solved in this case is a onedimensional, linear, selfadjoint eigenvalue problem of second order for a displacement vector $\vec{\xi}$ with three components ξ_r, ξ_θ, ξ_z. It can be shown analytically that the full spectrum of eigenvalues may contain continuous parts [5, 6], accumulation points [4] or distinct infinitely degenerate eigenvalues [4]. So it is not astonishing that the standard choices of basis functions [1 - 4], e.g. piecewise linear or cubic functions for all components of $\vec{\xi}$, may not be the best. In fact, the choice of linear basis functions destroys the degeneracy of the Alfvenoscillations in a homogeneous currentless plasma cylinder [4]. The corresponding numerical results have a Bessel-function-like shape, which is attributable to the discretization and not to physics. The same discretization errors make it impossible to find the correct shape of the unstable modes in a fixed boundary Tokomak, although the eigenvalue of the most unstable mode can be obtained [2].

We shall show that all these defects of the method disappear if a more appropriate choice of the basis functions is made. Since the variational form of the eigenvalue problem contains only first derivatives of ξ_r [2], discontinuous basis functions are admissible for the components ξ_θ and ξ_z. Our choice then is determined by a physical argument. Because unstable modes are nearly incompressible, the displacement $\vec{\xi}$ should be approximated within a function class where incompressibility can well be represented. So we are led to a special combination of piecewise linear and piecewise constant basis functions. It is noteworthy that despite the use of simpler functions, the convergence properties are improved.

THE PHYSICAL PROBLEM

Consider a small, time and space dependent displacement $\vec{\xi}$ of a perfectly conducting fluid in magnetohydrostatic equilibrium. The equation of motion for $\vec{\xi}$ is given by [7]

$$\rho \frac{\partial^2 \vec{\xi}}{\partial t^2} = \vec{F}(\vec{\xi})$$

$$\equiv \vec{\nabla}(\vec{\xi}\cdot\vec{\nabla}p + \gamma p \vec{\nabla}\cdot\vec{\xi}) + (\vec{\nabla}\times\vec{Q})\times\vec{B} + (\vec{\nabla}\times\vec{B})\times\vec{Q} \qquad (1)$$

where $\vec{Q} = \vec{\nabla}\times(\vec{\xi}\times\vec{B})$. Here $\rho(\vec{r})$, $p(\vec{r})$ and $\vec{B}(\vec{r})$ denote equilibrium quantities, the mass density, the pressure and the magnetic field respectively. γ is the adiabaticity index. The equilibrium quantities satisfy the following relation

$$(\vec{\nabla}\times\vec{B})\times\vec{B} = \vec{\nabla}p \qquad (2)$$

A current way to attack the stability problem in an axisymmetric infinitely long plasma is to look for normal mode solutions

$$\vec{\xi}(\vec{r}) = \vec{\xi}(r)\, e^{i(\omega t + m\theta + kz)} \qquad (3)$$

of equation (1), constrained by the boundary conditions

$$\vec{\xi}(0) \text{ finite}, \quad \xi_r(R) = 0 \qquad (4)$$

where R is the radius of a bounding impenetrable wall. ξ_r, ξ_θ, ξ_z are the components of $\vec{\xi}$ in cylindrical coordinates. Under these assumptions the equation of motion (1) may be brought to the variational form of Newcomb [8], i.e. the stationary point formulation [9] of the eigenvalue problem

$$\omega^2 \delta \int \rho |\vec{\xi}|^2 r\,dr = \delta \int \left\{ \Lambda\left(\xi_r, \frac{d\xi_r}{dr}\right) + \gamma p \left| \eta + \frac{1}{r}\frac{d}{dr}(r\xi_r) \right|^2 + \frac{k^2 r^2 + m^2}{r^2} \left| \xi - \zeta_0\left(\xi_r, \frac{d\xi_r}{dr}\right) \right|^2 \right\} r\,dr \qquad (5)$$

where

$$\Lambda\left(\xi_r, \frac{d\xi_r}{dr}\right) = \frac{1}{k^2 r^2 + m^2}\left|\left(k_r B_z + m B_\theta\right)\frac{d\xi_r}{dr} + \left(k_r B_z - m B_\theta\right)\frac{\xi_r}{r}\right|^2 + \left[\left(k_r B_z + m B_\theta\right)^2 - 2 B_\theta \frac{d}{dr}\left(r B_\theta\right)\right]\frac{|\xi|^2}{r^2} \tag{6}$$

$$\xi_0\left(\xi_r, \frac{d\xi_r}{dr}\right) = \frac{r}{k^2 r^2 + m^2}\left[\left(k_r B_\theta - m B_z\right)\frac{d\xi_r}{dr} - \left(k_r B_\theta + m B_z\right)\frac{\xi_r}{r}\right] \tag{7}$$

$$\eta = i\frac{m}{r}\xi_\theta + ik\xi_z \tag{8}$$

$$\zeta = i\xi_\theta B_z - i\xi_z B_\theta \tag{9}$$

δ denotes the variation of a functional.

In (5) ξ_r , $i\xi_\theta$, $i\xi_z$ can be taken real without loss of generality [8] . Note that the left and the right hand sides of (5) are proportional to the kinetic and the potential energy of the plasma respectively. From (5) it is self-evident that the operator $\vec{F}(\xi)$ (1) is selfadjoint at least in the one-dimensional case (3), and is shown for the general case by Greene and Johnson [10] . Hence the eigenfrequencies ω^2 are real. The plasma is unstable when negative eigenvalues ω^2 exist. Note further that (5) contains only derivatives on ξ_r .

The energy principle (5) was the starting point of many analytical papers on MHD-stability in the last 15 years. In most cases the problem was significantly simplified by determining only the minimum of the potential energy rather than the full solution of the stationary point problem (5). This method (so called δW - method) will give the correct answer for marginal stability ($\omega = 0$), but cannot give correct growth rates as can be seen by the following considerations.

In the δW - method the second and the third term in the potential energy integral in (5) can be minimized to zero because the first term does not depend on ξ_θ and ξ_z . Hence minimum potential energy implies incompressibility (second term : div $\vec{\xi} = 0$) of the unstable modes. Since the adiabaticity index influences the motion (1), (5) only in the combination γ div $\vec{\xi}$, growth rates calculated with the δW - method do not depend on γ . On the other hand it is known [2, 11] that growth rates may strongly depend on γ . Therefore the δW - method is not appropriate when exact knowledge of the growth rates is required. Already Bernstein et al. [12] were aware of this fact when originally formulating their energy principle in 1958.

However, the δW - method gives us a hint how to choose our basis functions when attacking the full stationary point problem (5) with the method of finite elements. A weakly unstable displacement has small div $\vec{\xi}$ and small $\zeta - \zeta_0$ (5) - (9), since these two quantities are exactly zero in the marginal case ($\omega = 0$). Therefore, it should be possible to represent div $\vec{\xi} = 0$ and $\zeta - \zeta_0 = 0$ within the function class chosen. However, by comparison of numerical and analytic results, we did not find an indication that the latter condition should be satisfied whereas the first one is indispensable. To see why, we reexamine the spectrum of a plasma cylinder of constant density in a homogeneous longitudinal magnetic field B_z [4].
The equation of motion specialized to this case reads:

$$-\omega^2 \rho \xi_z = ik\gamma p \, \vec{\nabla} \cdot \vec{\xi}$$

$$-\omega^2 \rho \vec{\xi}_\perp = (B_z^2 + \gamma p)\vec{\nabla}_\perp(\vec{\nabla}\cdot\vec{\xi}) - ik B_z^2 (\vec{\nabla}_\perp \xi_z - ik\vec{\xi}_\perp) \qquad (8)$$

Here $\perp$ denotes vectors perpendicular to the magnetic field. ρ , p , B_z are constant. Obviously, $\vec{\nabla}\cdot\xi = 0$, $\xi_z = 0$, $(k^2 B_z^2 - \omega^2\rho)\vec{\xi}_\perp = 0$ yields solutions of (8), the so-called Alfven-oscillations. The eigenvalue $\omega^2 = k^2 B_z^2/\rho$ is infinitely degenerate, since every ξ_r satisfying the boundary condition (4) determines with $\vec{\nabla}\cdot\vec{\xi} = 0$ a non-trivial ξ_θ .

Imagine now a plasma with an additional small B_θ (e.g. Tokamak). It can be

shown [2, 13, 14] that, for special values of B_θ, the Alfven-oscillations go unstable. For a good discrete approximation of these instabilities we require the degenerate eigenvalue of the solution without B_θ to be exactly represented by the finite element method. With the method described in [4] we found one third of the eigensolutions to be bad Alfven-modes. An exact representation of the Alfven-modes can therefore be expected, if the discrete description of (8) allows to one third of the linearly independent solutions to exactly satisfy div $\vec{\xi} = 0$ and $\xi_z = 0$.

DISCRETIZATION

Let us carry out the variation (5) :

$$a(\delta\vec{\xi}, \vec{\xi}) - \omega^2 b(\delta\vec{\xi}, \vec{\xi}) = 0. \tag{9}$$

Then the problem to be solved may be formulated as follows: find a scalar ω^2 and a "sufficiently regular" vector $\vec{\xi}$ satisfying the boundary conditions (4), for which (9) holds whatever "sufficiently regular" $\delta\vec{\xi}$ satisfying (4) is taken.

In order to get rid of the apparent singularities induced in (5) by the cylindrical geometry we define a new displacement vector [16] $\hat{\vec{\xi}}$

$$\hat{\vec{\xi}} = \begin{pmatrix} \hat{\xi}_1 \\ \hat{\xi}_2 \\ \hat{\xi}_3 \end{pmatrix} = U \cdot \vec{\xi} = \begin{pmatrix} \xi_r \\ (\xi_r + im\xi_\theta)/r \\ i\xi_z \end{pmatrix} \tag{10}$$

All components of $\hat{\vec{\xi}}$ are real, because ξ_r, $i\xi_\theta$, $i\xi_z$ may be real. With (10) we exclude the case m = 0 from our further considerations. This case could be treated with the transformation used in [4]. Let us further define

$$\hat{a}(\delta\hat{\vec{\xi}}, \hat{\vec{\xi}}) = a(U^{-1}\delta\hat{\vec{\xi}}, U^{-1}\hat{\vec{\xi}}) \quad \text{and} \quad \hat{b}(\delta\hat{\vec{\xi}}, \hat{\vec{\xi}}) = b(U^{-1}\delta\hat{\vec{\xi}}, U^{-1}\hat{\vec{\xi}}).$$

Then the problem to be solved is given by (9), if everywhere the hat is inserted. We will use the obvious notation $(\hat{9})$. The essential structure of the bilinear forms a and $\hat{a}$ is the same: they only contain first derivatives d/dr on $\vec{\xi}$ and $\hat{\xi}_1$ respectively. Hence "sufficiently regular" means that $\vec{\xi}$ belongs to $H = H^1(o,R) \times L_2(o,R) \times L_2(o,R)$, i.e., $\hat{\xi}_1$ belongs to the Sobolev space $H^1(o,R)$ and that $\hat{\xi}_2$ and $\hat{\xi}_3$ are square integrable.

For the numerical treatment of $(\hat{9})$ we need a finite-dimensional (dimension N) subspace V of "sufficiently regular" functions $\vec{\xi}$ with the property explained in the preceding section: V should contain N/3 linearly independent functions $\vec{\xi}$ satisfying

$$\left.\begin{aligned} \vec{\nabla}\cdot\vec{\xi} = \vec{\nabla}\cdot U^{-1}\hat{\vec{\xi}} = \frac{d\hat{\xi}_1}{dr} + \hat{\xi}_2 + \hat{\xi}_3 = 0 \\ \hat{\xi}_3 = 0 \end{aligned}\right\} \qquad (11)$$

in every point of the interval $0 \leq r \leq R$.

More accurately V can be defined in the following way.

Let V_1 be a finite-dimensional subspace of $H^1(o,R)$ of type "finite element" constrained by the boundary conditions (4). Let V_2 and V_3 be two finite-dimensional subspaces of $L_2(o,R)$ and having the properties: For all $\hat{\xi}_1 \in V_1$ there exists $\hat{\xi}_2 \in V_2$ and $\hat{\xi}_3 \in V_3$ such that $\frac{d\hat{\xi}_1}{dr} + \hat{\xi}_2 + \hat{\xi}_3 = 0$. V is then defined by $V = V_1 \times V_2 \times V_3$.

Let us first examine the subspaces of "sufficiently regular" functions used in [1 - 4]. Assume the interval $0 \leq r \leq R$ to be divided in n subintervals. A piecewise linear (i.e. linear in every subinterval), continuous function is determined by 3n + 1 nodal values: n + 1 nodal values for each component of $\vec{\xi}$ minus the two determined by the boundary condition (4). Hence the dimension of the space is N = 3n + 1. The number of constraints given by (11) is also 3n + 1, since the n + 1 nodal values of $\hat{\xi}_3$ and the n pieces of the piecewise linear function $d\hat{\xi}_1/dr + \hat{\xi}_2$ have to be identically zero. Consequently no piecewise linear, continuous function $\vec{\xi}$ satisfying (11) exists. Almost the same is true for piecewise cubic, continuous functions with continuous first derivatives. In this case, the dimension is N = 6n + 4 and the number of constraints is 6n + 2. At most two linearly independent functions may satisfy (11).

From all possible subspaces V, which contain N/3 linearly independent functions satisfying (11) we choose the simplest one: continuous piecewise linear $\hat{\xi}_1$ and piecewise constant $\hat{\xi}_2$ and $\hat{\xi}_3$. In this space of dimension 3n - 1 the condition (11) yields 2n constraints. Hence n - 1 "good" Alfven-modes may exist. The basis of V is given by

$$\begin{pmatrix} e_i \\ 0 \\ 0 \end{pmatrix}, i = 0, 1, \dots, n ; \begin{pmatrix} 0 \\ c_{i+1/2} \\ 0 \end{pmatrix}, \begin{pmatrix} 0 \\ 0 \\ c_{i+1/2} \end{pmatrix}, i = 0, 1, \dots, n-1 \qquad (12)$$

where e_i are triangular functions as defined in [4] and

$$c_{i+1/2}(r) = \begin{cases} 1 \text{ for } r_i < r < r_{i+1} \\ \\ 0 \text{ elsewhere} \end{cases} \qquad 0 \leq i < n-1 \qquad (13)$$

Here a mesh $0 = r_0 < r_1 < \dots < r_n = R$ is assumed. The approximation of a displacement $\vec{\xi}$ in the space V reads

$$\vec{\xi} = \sum_{i=0}^{n} x_1^i \begin{pmatrix} e_i \\ 0 \\ 0 \end{pmatrix} + \sum_{i=0}^{n-1} \left[x_2^{i+1/2} \begin{pmatrix} 0 \\ c_{i+1/2} \\ 0 \end{pmatrix} + x_3^{i+1/2} \begin{pmatrix} 0 \\ 0 \\ c_{i+1/2} \end{pmatrix} \right] \qquad (14)$$

where the nodal parameters x_1^i , $x_2^{i+1/2}$, $x_3^{i+1/2}$ are the values of $\hat{\xi}_1$ at $r = r_i$ and of $\hat{\xi}_2$ and $\hat{\xi}_3$ at $r = r_{i+1/2} \equiv (r_i + r_{i+1}) / 2$. The insertion of (14) for $\vec{\xi}$ and (12) for $\delta\vec{\xi}$ in ($\hat{9}$) yields together with (4) an algebraic eigenvalue problem of dimension 3n - 1. The integrals (5) necessary to be carried out to this end may be performed by using a Simpson-routine.

APPLICATIONS

The homogeneous currentless plasma cylinder

First we apply our method to the simple situation described by equation (8). With a mesh of n intervals, we find the eigenvalue $\omega^2 = B_z^2 k^2/\rho$ to be (n - 1) - fold degenerate in contrast to [4]. Because of the degeneracy, no spurious physical structure of the associated eigenvectors as in [4] was observed. These two results were our principle goal when introducing the space V (12).

There was a second class of badly described eigensolutions in our previous work, the slow waves, whose eigenvalues are analytically given by:

$$\omega_\alpha^2 = \frac{B_z^2}{2\rho R^2}\left(R^2k^2+\gamma_{m,\alpha}^2\right)\left(1+s^2\right)\left[1-\sqrt{1-\frac{4s^2}{(1+s^2)^2}\,\frac{R^2k^2}{R^2k^2+\gamma_{m,\alpha}^2}}\right] \qquad (15)$$

where $s^2=\gamma p/B_z^2$ and $\gamma_{m,\alpha}$ is the α^{th} zero of $dJ_m(x)/dx$. With increasing α, i.e. increasing $\gamma_{m,\alpha}$, ω_α^2 decreases and tends towards the accumulation point $\omega_\infty^2 = \gamma p\, k^2/\rho(1+s^2)$. The frequency band occupied by this class of solutions may be very narrow relative to the value of the accumulation point, which is, in addition, the lowest frequency of the whole spectrum. Fig. 1 shows the numerical solution to (15) as a function of the number n of intervals. The parameters used are m = 1, k = 0.5 and s^2 = 1/12 (plasma with β = 0.1 and γ = 5/3).

The modes corresponding to this spectrum are well described; once more in contrast to [4]. As an example, we compare in Fig. 2 the numerical solutions for the modes corresponding to ω_4^2 and ω_8^2 with the analytic solutions $J_1(\gamma_{1,4}\, r/R)$ and $J_1(\gamma_{1,8}\, r/R)$ respectively. In [4] the mode associated with ω_2^2 was badly described, whereas the higher modes could even not be identified. Note that these results can only be obtained in the space V as specified by (12), whereas the Alfven-class would be degenerate even with linear, continuous ξ_z, since $\xi_z(r)=0$ for this class.

The inhomogeneous currentless plasma cylinder (continuous spectra)

This is a simple plasma model which exhibits singular eigenmodes of the two kinds [6] possible in a general screw-pinch. The model is characterized by

$$B_z = \text{const},\ B_\theta = 0,\ p = \text{const} \quad \text{and} \quad \rho = \rho_0\left[1 - \epsilon\,(r^2/R^2)\right], \quad \text{where } 0 \leq \epsilon \leq 1 \tag{16}$$

Equation (8) still holds for this plasma. Let us eliminate ξ_θ and ξ_z from (8). We then find [11]

$$\frac{d}{dr}\left[\frac{b_A(r)\, b_s(r)}{N(r)}\,\frac{1}{r}\,\frac{d}{dr}(r\xi_r)\right] + b_A(r)\,\xi_r = 0 \tag{17}$$

where

$$\left.\begin{aligned} b_A(r) &= \rho(r)\,\omega^2 - k^2 B_z^2 \\ b_s(r) &= \rho(r)\,\omega^2\,(\gamma p + B_z^2) - k^2 B_z^2\,\gamma p \\ N(r) &= \rho^2(r)\,\omega^4 - \left(k^2 + \frac{m^2}{r^2}\right) b_s(r) \end{aligned}\right\} \tag{18}$$

Equation (17) has solutions with logarithmic singularities at points r_A and r_s, if somewhere in the interval $0 < r < R$ $b_A(r_A) = 0$ or $b_s(r_s) = 0$. The equation is of Fuchs' type in the neighborhood of such a point. On the other hand, it can be shown [6] that $N(r) = 0$ does not give rise to singular solutions. Note that $b_A(r) = 0$ yields the dispersion relation for the Alfven-class in the limiting case of constant density ($\epsilon = 0$). Similarly, $b_s(r) = 0$, $\epsilon = 0$ yields the accumulation point ω_∞^2 of the slow waves. Further, by expressing ξ_θ and ξ_z (8) in terms of ξ_r, it can be shown, that ξ_θ exhibits a singularity $(r - r_A)^{-1} \ln|r - r_A|$ at the points $b_A(r_A) = 0$ and ξ_z in turn a singularity $(r - r_s)^{-1} \ln|r - r_s|$ at the points $b_s(r_s) = 0$.

At first glance, one might be puzzled by the existence of singular normal modes. But remember that we are calculating Fourier transforms (3) of physical quantities and that a Fourier transform of a well-behaved function may be a distribution, e.g. $\delta(x - \omega)$ is the transform of exp(ixt). In fact, these singular normal modes with divergent $\int |\vec{\xi}|^2 \, r\,dr$ are not meaningless, if they are associated with a continuous spectrum, which allows well-behaved square-integrable wave-packets to form. Such continua do exist, since every point, where $b_A(r) = 0$ or $b_s(r) = 0$, gives rise to a singular solution, which satisfies the boundary condition [17, 18]. The two continua are given by

$$\text{Alfven} \quad \min_{0<r<R} \frac{k^2 B_z^2}{\rho(r)} \leq \omega^2 \leq \max_{0<r<R} \frac{k^2 B_z^2}{\rho(r)} \tag{19}$$

$$\text{Slow wave} \quad \min_{0<r<R} \frac{k^2 \gamma p}{\rho(r)(1+s^2)} \leq \omega^2 \leq \max_{0<r<R} \frac{k^2 \gamma p}{\rho(r)(1+s^2)} \tag{20}$$

So, the inhomogeneous density distribution spreads the degenerate eigenvalues of the Alfven-waves and the accumulation point of the slow waves to form continua. Having been successful in the numerical approximation of these two special points in the spectrum of the plasma with homogeneous density, we wondered, how continua and singular modes would be approximated by the finite element method. A reason why we are looking at these singular modes is the fact that localized regular unstable Suydam-modes, as they appear in a diffuse pinch with current flow, behave quite similarly. Naturally, the maximum number of modes associated with a "continuum" is given by the number of mesh-points, where "singularities" may arise. In our model, we find n - 1 Alfven-modes and $n - n_d - 1$ slow modes, where n_d denotes the number of slow modes associated with discrete eigenvalues. First we show in Fig. 3 how the "singularity" of an Alfven-mode grows, when the number n of intervals is increased. The density parameter ϵ (16) is chosen to be 0.1. The modes are normalized

$$\int_0^1 |\vec{\xi}|^2 \, r\,dr = 1 \tag{21}$$

numerically. The components $\hat{\xi}_1 = \xi_r$ and $\hat{\xi}_3 = i\xi_z$ being much smaller than the component $\hat{\xi}_2 = (\xi_r + im\xi_\theta)/r$, Fig. 3 shows only the component $\hat{\xi}_2$. The $1/(r - r_A)$ behaviour of the mode can clearly be seen. Its maximum amplitude increases ($\propto \sqrt{n}$) and its half-width decreases ($\propto 1/n$) with increasing n since no norm for the analytic solution exists:

$$\int_0^R |\xi_\theta|^2 \, r\,dr \propto \int_0^R \left[\frac{\ln|r-r_A|}{r-r_A}\right]^2 r\,dr = \infty \tag{22}$$

Satisfied by our diverging modes, we were sure that this phenomenon takes place at the right point. Fig. 4 shows for $\epsilon = 0.1$ the frequencies (normalized with $\omega_0^2 \equiv k^2 B_z^2 / \rho_0$) of all Alfven-modes possible with n intervals in function of the radius r_A, where their "singularity" is situated. To every point of localization of the numerically determined eigenfunction, we have added an error bar with the length of two intervals of the mesh used. The solid line represents the analytic solution $b_A(r_A) = 0$, i.e. $\omega^2/\omega_0^2 = 1/(1 - \epsilon r_A^2)$.

From Figs. 3 and 4, we conclude that a numerical spectrum may be regarded as continuous in a certain frequency band, if

1° the associated normalized modes have "singularities" in distinct points r_A ;

2° the number of such modes increases in a fixed interval with increasing number of mesh points ;

3° the polygon defined by the location r_A and the associated frequency ω^2 of the modes converges to a smooth curve.

As a further demonstration (Fig. 5), we calculate the spectrum of the slow waves. With increasing inhomogeneity, i.e., increasing ϵ (16), the accumulation point

opens to a continuum which eventually covers the discrete eigenvalues. The solid line represents the analytic upper limit (20) of the continuum.

A simple screw-pinch model

Finally we apply our method to an imcompressible plasma ($\gamma = \infty$) of constant density ϱ lying in a constant longitudinal field B_z and carrying a longitudinal, constant current. The pressure p satisfies the pressure balance (2). The stability theory of such a plasma was given by Shafranov [19] for $m \gg 1$. Takeda et al. [2] tested their finite element method with this model and found that there might be an error inherent in the numerical formulation. Yet, taking a large number of mesh-points they were successful in calculating the growth rates of the most unstable modes. We shall show that the discrete space V (12) should be chosen rather than the space chosen by Takeda et al. [2], if good accuracy is desired. Further we shall show that the unstable modes are well approximated within a low-dimensional space V, whereas it is almost impossible to approximate them within the space chosen by Takeda et al. [2].

First we quote Shafranov's result for the component ξ_r of an unstable mode

$$\xi_r = \text{const.} \left\{ \frac{m}{r} (\mu+1) J_m (kr\sqrt{\mu^2-1}) - k\sqrt{\mu^2-1}\, J_{m-1} (kr\sqrt{\mu^2-1}) \right\} \quad (23)$$

Here $\mu = 2k^2\tau/\sigma\left(k^2\tau^2 - \omega^2\varrho/B_z^2\right)$, $\tau = 1 - m/\sigma$ and $\sigma = k R B_z / B_\theta(R)$. The boundary condition (4) is satisfied for values μ_0, which determine the growth rates of the modes

$$-\omega^2 = \frac{B_z^2 k^2}{\varrho} \left(\frac{2\tau}{\mu_0 \sigma} - \tau^2 \right) \quad (24)$$

Fig. 6 now shows the results for the growth rates (m = 2, k = - 0.2) obtained by Takeda's and by our method. In both cases, we used an equidistant mesh of 20 intervals. With all linear and continuous basis functions a single unstable mode can be found, whereas in space V there are more than 10. The growth rates of the 6 most unstable modes (strictly speaking mode-pairs) are drawn. They correspond to the following 6 pairs of μ_0 - values: - 25.19, 26.19; - 41.60, 42.59; - 73.49, 74.48; - 89.31, 90.30; - 105.09, 106.09; - 120.86, 121.85. The solid lines represent the analytic solution (24). In Fig. 7, then, the analytic and the numerical solutions to the mode-form are compared. Once more, our elements and 20 intervals have been used. Figs. 6 and 7 demonstrate the good accuracy obtained with the finite element method satisfying conditions (11). From Fig. 6 one concludes that the error inherent in the numerical formulation of Takeda et al. [2] is caused by the violation of these conditions.

CONCLUSIONS

We have proposed a new class of very simple basis functions for the finite element approximation of the one-dimensional normal mode MHD-equations. It has been shown that within this function class certain important features of the fixed boundary MHD-problem are exactly or at least intelligibly described by the discrete system. The proposed basis functions are appropriate for extremely local instabilities [15] in complicated equilibrium conditions. They allow to calculate singular eigenmodes having a continuous spectrum (section IV) and they even describe correctly the eigenvalues and eigenfunctions of the slow waves (section IV), i.e. a class of solutions of (8) with discrete eigenvalues in an extremely narrow frequency band, which are descending towards an accumulation point [4] . Finally, we showed that the instabilities of a screw-pinch with fixed boundary can be calculated with high accuracy even using few mesh-points.

Originally, the choice of the new basis functions was motivated by our desire to describe the instabilities of a screw-pinch more accurately. Afterwards, we found them to be much more universal. So we believe that they could be useful in free boundary MHD and in other branches of physics and engineering as well. We do not

intend to give criteria for their applicability, but we would like to give the following hint: If the variational form of your finite element problem at hand admits a discontinuous basis, try it.

ACKNOWLEDGEMENTS

We are indebted to Dr. R.A. Dory and Dr. F. Hofmann who have carefully read and criticized the manuscript. We would also like to thank Prof. Dr. J. Descloux and Dr. F. Troyon for their helpful comments and discussions.

This work was supported by the Swiss National Science Foundation.

REFERENCES

1 M. Ohta, Y. Shimomura, T. Takeda, Nucl. Fus. 12, 271 (1972)

2 T. Takeda, Y. Shimomura, M. Ohta and M. Yoshikawa, Phys. Fluids 15, 2193 (1972)

3 T.J.M. Boyd, G.A. Gardner and L.R.T. Gardner, Nucl. Fus. 13, 764 (1973)

4 K. Appert, D. Berger, R. Gruber, F. Troyon, J. Rappaz, ZAMP 25, 229 (1974)

5 H. Grad, Proc. Nat. Acad. Sci. USA, 70, 3277 (1973)

6 K. Appert, R. Gruber, J. Vaclavik, Phys. Fluids, accepted for publication

7 G. Schmidt, "Physics of High Temperature Plasmas", Academic Press , New York , 1966

8 W.A. Newcomb, Annals of Physics, 10, 232 (1960)

9 G. Strang and G.J. Fix, "An Analysis of the Finite Element Method", Prentice-Hall, Inc., Englewood Cliffs, N.J., 1973

10 J.M. Greene and J.L. Johnson, Hydromagnetic Equilibrium and Stability, in "Advances in Theoretical Physics" (K.A. Brueckner, ed.) Vol. 1, p. 195, Academic Press, New York / London, 1965

11 J.P. Goedbloed and H.J.L. Hagebeuk, Phys. Fluids 15, 1090 (1972)

12 I.B. Bernstein, E.A. Frieman, M.D. Kruskal and R.M. Kulsrud, Proc. Roy. Soc. A 244, 39 (1958)

REFERENCES (Cont.)

13 V.D. Shafranov, Sov. Phys. Tech. Phys. 15, 175 (1970)

14 K. Appert, D. Berger, R. Gruber, J. Rappaz and F. Troyon ZAMP 25, 116 (1974)

15 K. Appert, D. Berger and R. Gruber, Physics Letters 46A, 339 (1974)

16 K. Appert, D. Berger and R. Gruber, LRP 76/73, Ecole Polytechnique Fédérale de Lausanne, Centre de Recherches en Physique des Plasmas

17 J. Tataronis and W. Grossmann, Zeitschrift f. Physik 261, 203 (1973)

18 E.M. Barston, Annals of Physics 29, 282 (1964)

19 V.D. Shafranov in "Plasma Physics and the Problem of Controlled Thermonuclear Reactions", Vol. IV, p. 71, Pergamon Press, London 1960.

FIGURE CAPTIONS

Fig. 1 : Numerically calculated spectrum of the slow wave branch in the homogeneous currentless plasma cylinder as a function of the number of intervals. At right hand side the first 19 eigenvalues of the exact analytic spectrum are plotted. The wave numbers are $m = 1$, $k = -0.5$.

Fig. 2 : Analytic (solid line) and numerical (points) solution to the component $\hat{\xi}_3$ of the slow wave branch. The corresponding eigenvalues are $\omega_4^2 - \omega_\infty^2 = 2.5 \cdot 10^{-6}$ and $\omega_8^2 - \omega_\infty^2 = 5.8 \cdot 10^{-7}$ respectively. The boundary conditions have been used for the innermost point.

Fig. 3 : "Singular" Alfven eigenmodes of the inhomogeneous currentless plasma cylinder with 5, 10, 20 and 40 intervals. Only the dominant component $\hat{\xi}_2$ is given. r_A denotes the analytically determined position of the "singularity".

Fig. 4 : Numerically detected "continuous" spectrum of the Alfven branch for a density profile with $\varepsilon = 0.1$.

Fig. 5 : For an inhomogeneous currentless plasma cylinder with varying density profile ε, we show the frequency spectrum for the slow wave branch. The wave numbers are $m = 1$ and $k = -0.5$. The solid line represents the analytic limit between the discrete spectrum (upper part) and the continuous spectrum (lower part). At left hand side the analytic and the numerical spectrum are given for $\varepsilon = 0$.

FIGURE CAPTIONS (Cont.)

Fig. 6 : Growth rates versus σ of an incompressible screw-pinch carrying a homogeneous current. The solid lines represent the 6 most unstable mode pairs as obtained analytically from (24). The corresponding numerical results are indicated by points. At left hand side Takeda's method was used.

Fig. 7 : Analytic (solid line) and numerical (points) solutions to the radial component ξ_r of the 2 dominant unstable modes at $\sigma = 1.98$.

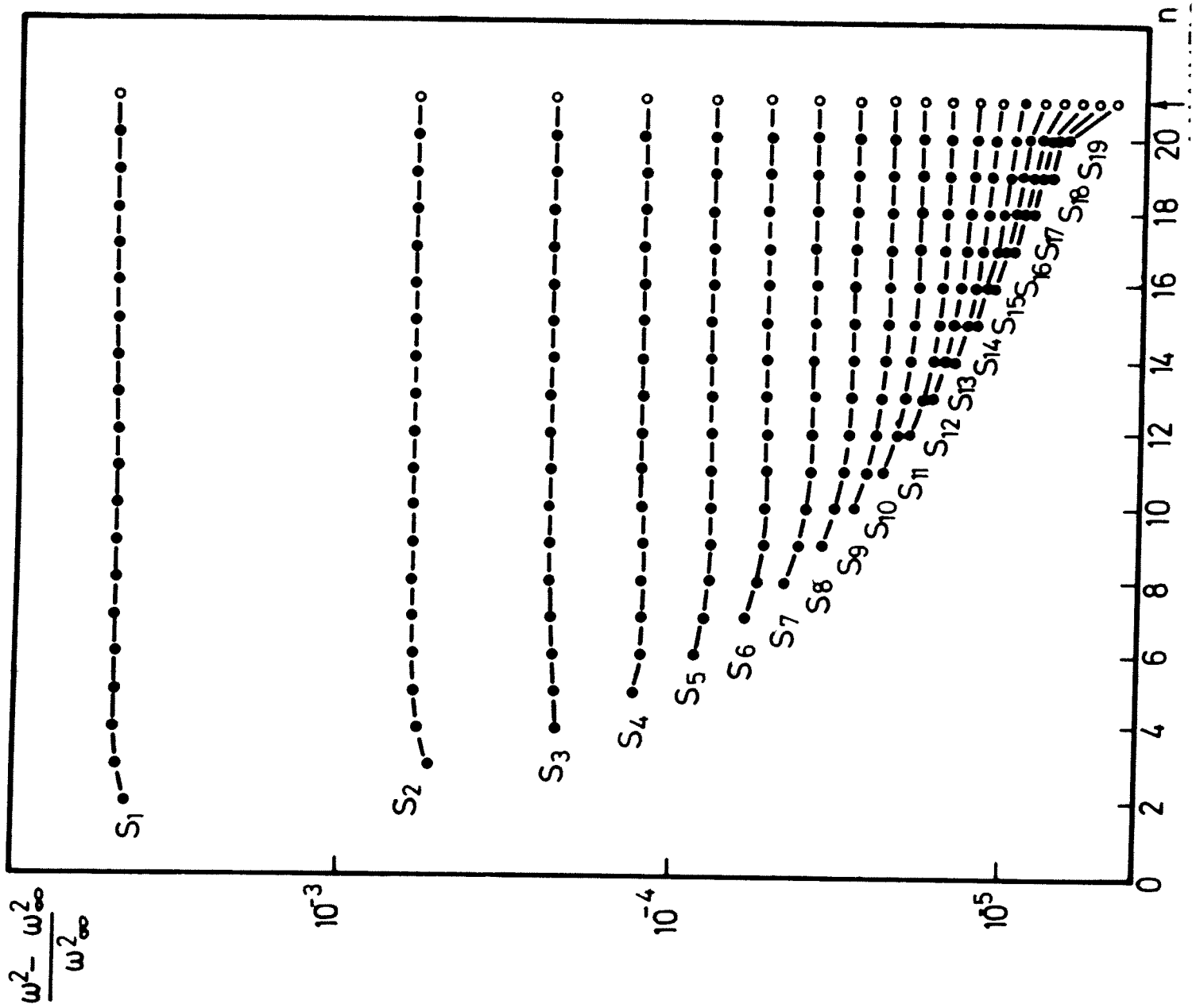
$\frac{\omega^2 - \omega_\infty^2}{\omega_\infty^2}$
10^{-3}
10^{-4}
10^{-5}
0
2
4
6
8
10
12
14
16
18
20
n
S_1
S_2
S_3
S_4
S_5
S_6
S_7
S_8
S_9
S_{10}
S_{11}
S_{12}
S_{13}
S_{14}
S_{15}
S_{16}
S_{17}
S_{18}
S_{19}

Figure 1

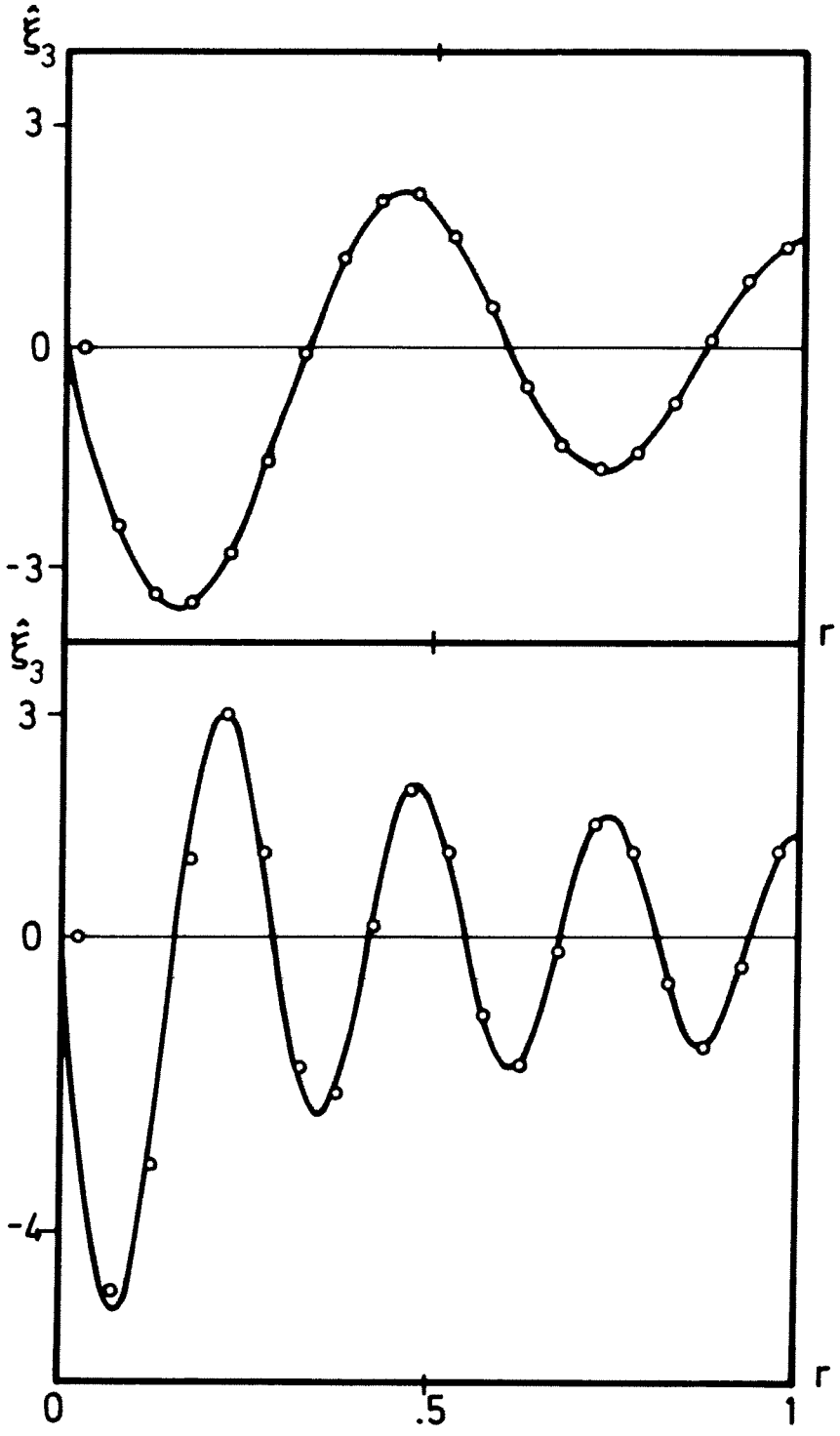

Figure 2

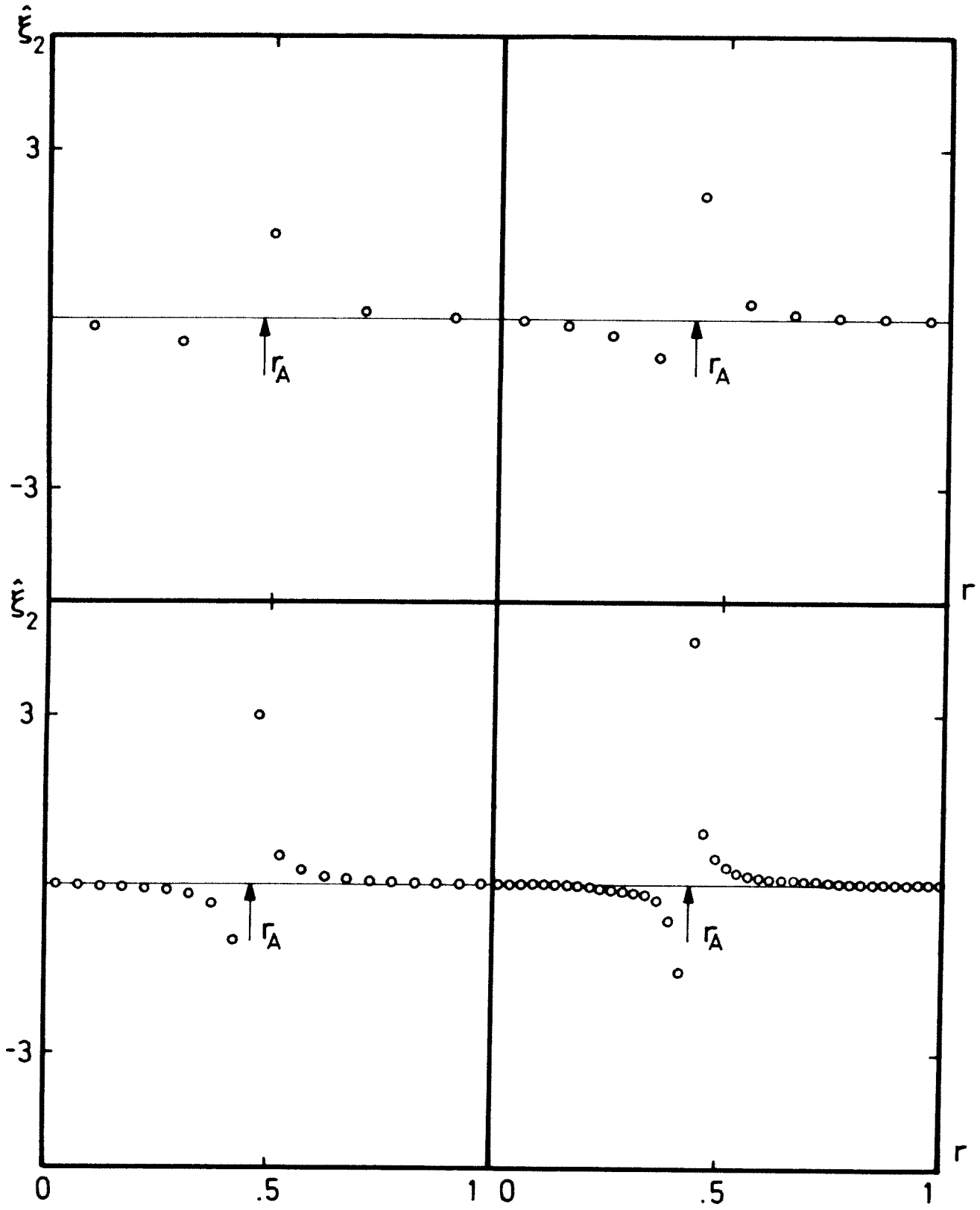

Figure 3

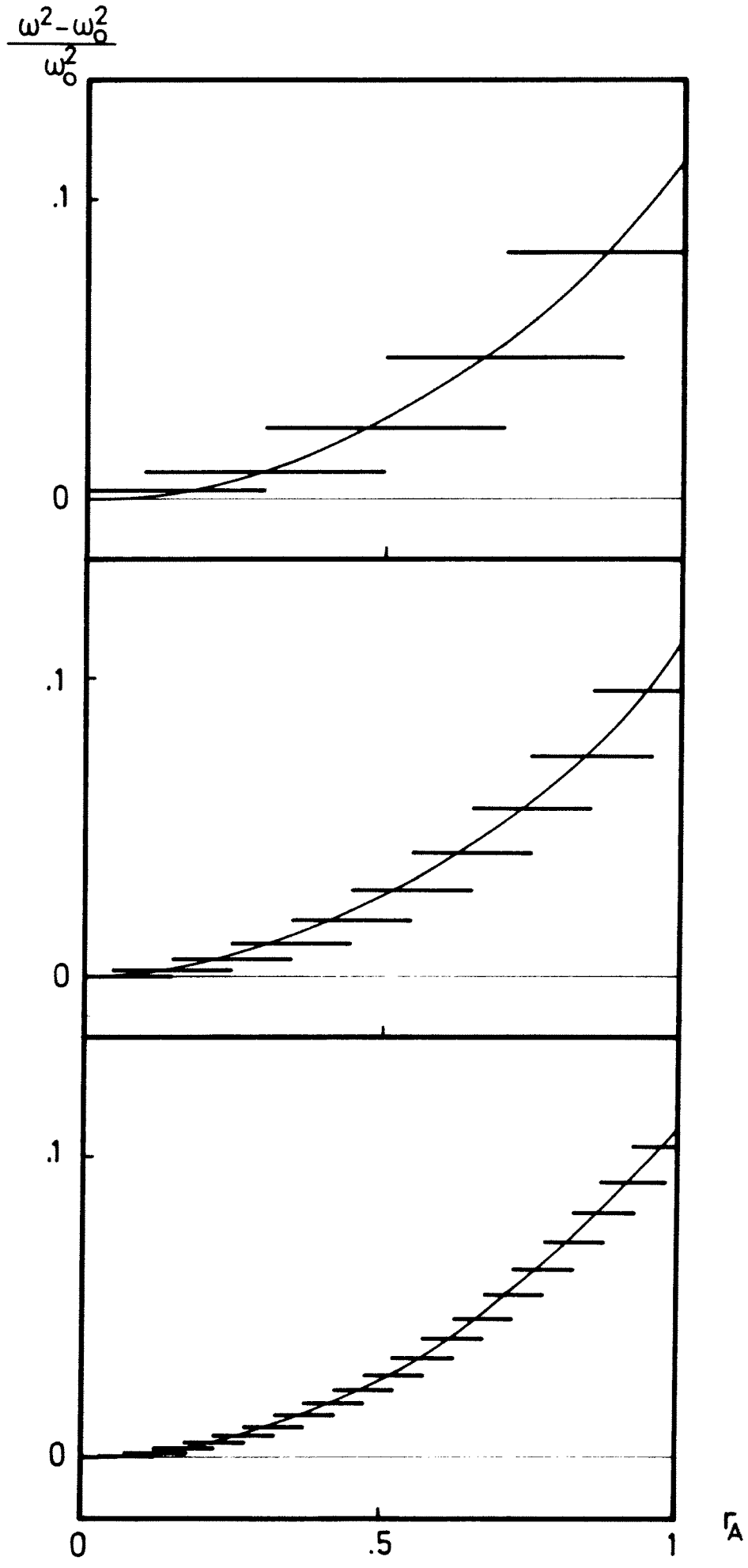

Figure 4

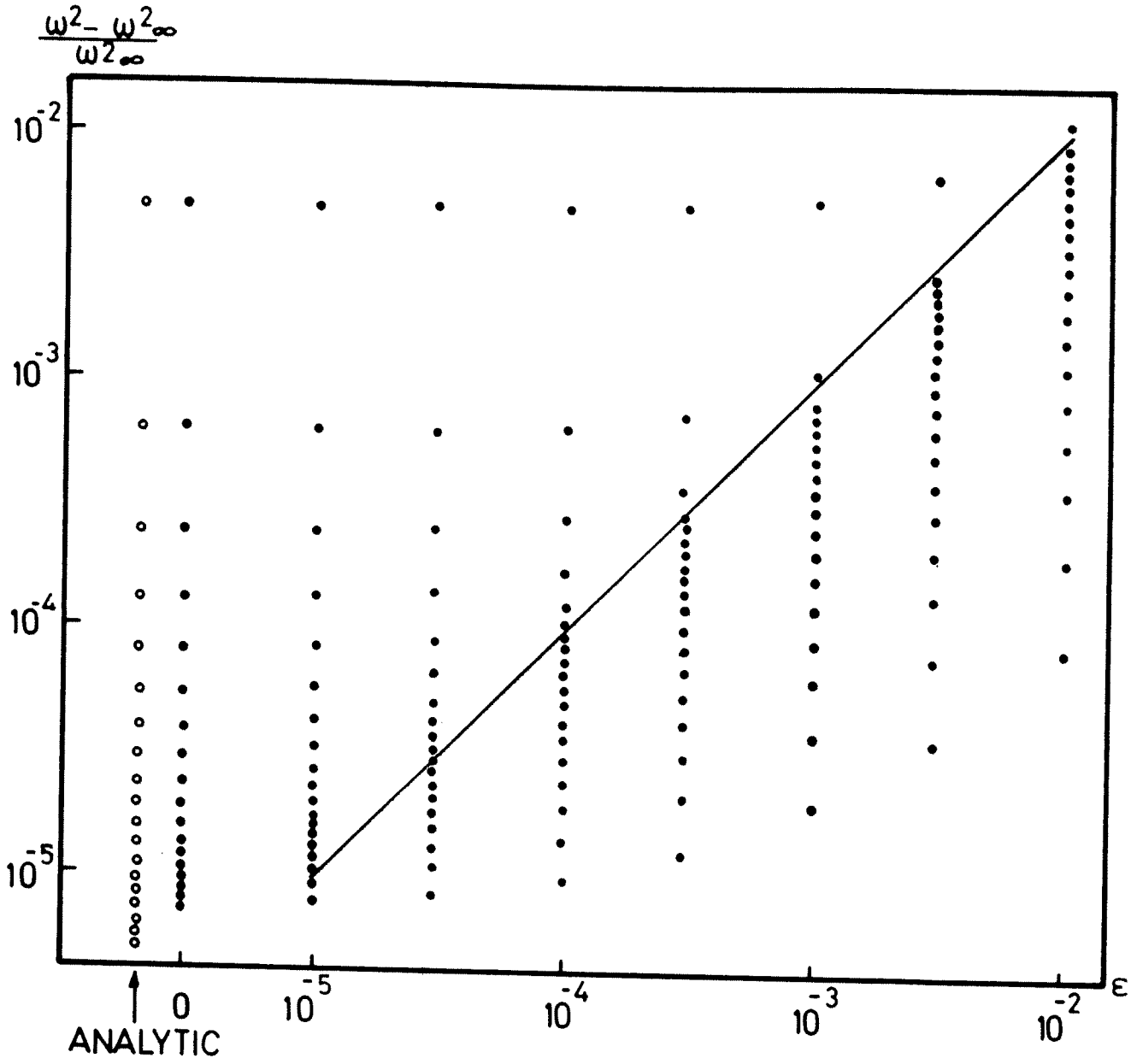
$\frac{\omega^2 - \omega^2_\infty}{\omega^2_\infty}$
10^{-2}
10^{-3}
10^{-4}
10^{-5}
0
ANALYTIC
10^{-5}
10^{-4}
10^{-3}
10^{-2}
ε

Figure 5

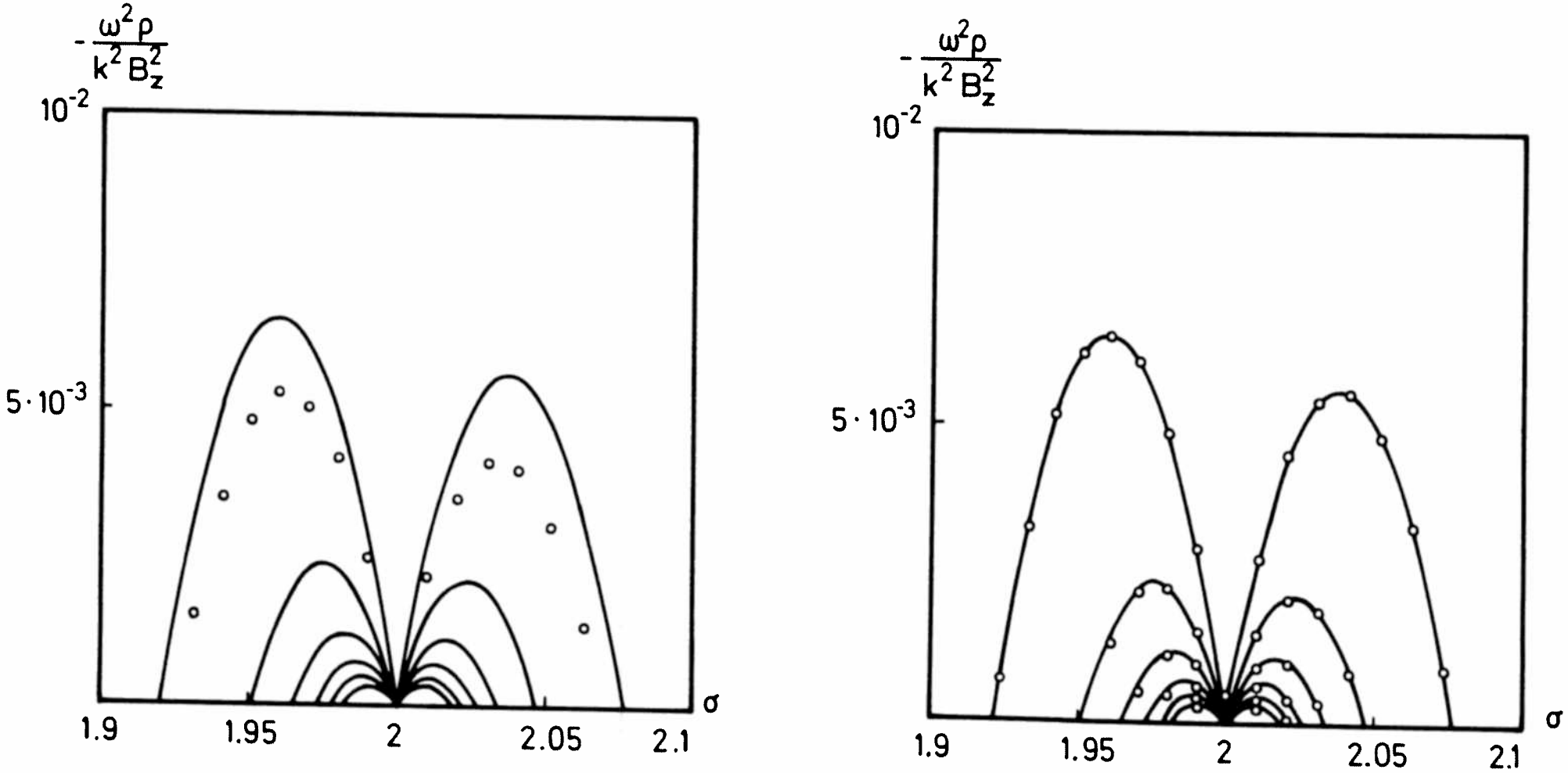
$-\frac{\omega^2\rho}{k^2 B_z^2}$
10^{-2}
$5\cdot10^{-3}$
1.9
1.95
2
2.05
2.1
σ
$-\frac{\omega^2\rho}{k^2 B_z^2}$
10^{-2}
$5\cdot10^{-3}$
1.9
1.95
2
2.05
2.1
σ

Figure 6

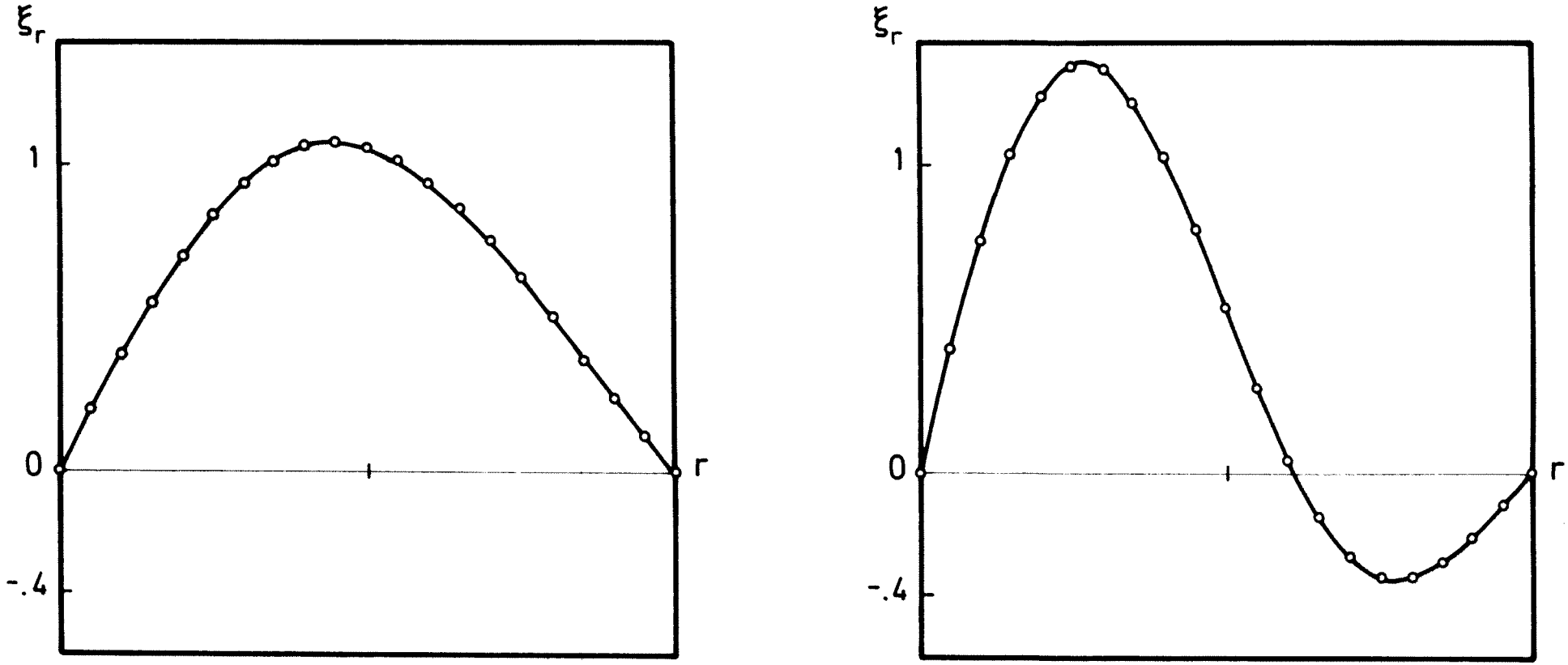

Figure 7

E R R A T A

Page 4: $k_r \equiv k \cdot r$